Characterization of the Reversible Taxol-Induced Polymerization of Plant Tubulin into Microtubules†

Carol L. Bokros, Jeffrey D. Hugdahl, Virginia R. Hanesworth, Jaitra V. Murthy, and Louis C. Morejohn*

Department of Botany, University of Texas at Austin, Austin, Texas 78713

Received August 12, 1992; Revised Manuscript Received November 24, 1992

ABSTRACT: Taxol has been reported to induce the polymerization of plant tubulin into microtubules, albeit weakly when compared to that of mammalian tubulin [Morejohn, L. C., & Fosket, D. E. (1984) *J. Cell Biol. 99*, 141–147], suggesting that taxol, a product of plant secondary metabolism, may interact poorly with plant microtubules. To test this idea in detail, we have investigated critical parameters affecting taxol-dependent microtubule polymerization and stability using tubulins from model cell lines of maize [*Zea mays* cv. Black Mexican Sweet (BMS)] and tobacco [*Nicotiana tabacum* cv. Bright Yellow 2 (BY-2)]. When plant tubulin dimer is isolated by using a modified version of the original method [Morejohn, L. C., & Fosket, D. E. (1982) *Nature 297*, 426–428], most of the tubulin polymerizes at 25 °C, with critical dimer concentrations (C_c) of 0.06 mg/mL for BMS tubulin and 0.13 mg/mL for BY-2 tubulin. When taxol-induced assembly is initiated with a 0–25 °C temperature jump, 42% of polymer is polymorphic, presumably due to aberrant nucleation events. Taxol-induced assembly at 2 °C minimizes the formation of polymorphic structures and is much more rapid than that of purified bovine brain tubulin, indicating a functional difference in the polymerization domains of these diverse tubulins. Temperature ramping during taxol-induced polymerization affords ≥95% assembly of plant tubulin into polymer consisting of 86% microtubules, which may be completely depolymerized by a combined treatment with low temperature and Ca^{2+}. We report for the first time that plant tubulin may be subjected to numerous cycles of efficient taxol-induced polymerization and cold/Ca^{2+}-induced depolymerization with little loss of polymerization competence. Gel filtration chromatography at low temperature may be used to separate taxol from soluble plant tubulin dimer, which retains its characteristic polymerization and herbicide-binding properties. Our results demonstrate that despite its origin from plants, taxol is a potent drug for the reversible polymerization of plant microtubules.

Microtubules are filamentous structures found in virtually all eukaryotic cells. Microtubules are composed mainly of tubulin, a heterodimeric protein having similar α- and β-subunits, each with a molecular mass near 50 kDa. In the presence of GTP[1] tubulin polymerizes in a head-to-tail fashion to form protofilaments, 13 of which form the basic microtubule wall. The extent of microtubule polymerization is dependent upon a critical concentration (C_c) of tubulin dimer, below which tubulin assembly will not spontaneously occur, and the mass of polymer formed above the C_c increases with the tubulin concentration (Dustin, 1984).

Taxol, a taxane alkaloid produced by plants within the genus *Taxus* (Wani et al., 1971), has been used to enhance the polymerization of microtubules in mammalian brain supernatant, a rich source of microtubule proteins (Vallee, 1982). Taxol lowers the C_c for mammalian microtubule polymerization (Schiff et al., 1979) and binds to polymerized tubulin rather than to free dimer (Parness & Horwitz, 1981; Takoudju et al., 1988). [^{3}H]Taxol binds to calf brain microtubules with K_d = 8.7 μM, and the molar binding stoichiometry of [^{3}H]taxol and brain tubulin is 0.78, indicating that one high-affinity, taxol-binding site exists on the polymerized dimer (Parness & Horwitz, 1981). Direct photoaffinity labeling experiments show preferential binding of [^{3}H]taxol to the β-subunit of calf brain tubulin (Rao et al., 1992). Taxol-treated animal microtubules have reduced treadmilling activity (Kumar, 1981; Caplow & Zeeburg, 1982) and are resistant to cold- or Ca^{2+}-induced depolymerization (Schiff et al., 1979; Kumar, 1981), although they depolymerize gradually when treated with a combination of cold and Ca^{2+} (Collins & Vallee, 1987). This reversibility of taxol-induced animal microtubule polymerization has been exploited for MAP isolation from animal cells (Collins & Vallee, 1987). A major advantage to the use of taxol exists in cases where the amounts of microtubule protein in extracts are limited. For example, taxol has been used to enhance the yield of microtubules and MAPs from HeLa cells and sea urchin eggs (Vallee, 1982; Vallee & Bloom, 1983; Collins & Vallee, 1987). Apparently taxol does not compete with MAPs in binding to animal microtubules (Vallee, 1982; Collins & Vallee, 1987).

In plants, microtubules participate in a number of critical subcellular functions, including chromosome migration during mitosis, cell plate formation during cytokinesis, and the orientation of cellulose microfibril deposition during cell wall formation (Fosket, 1989). Although most of our knowledge of tubulin biochemistry and pharmacology has come from extensive studies on mammalian microtubule systems (Dustin, 1984), very little information exists on the biochemical and pharmacological properties of plant tubulin and microtubules.

† This work was supported by National Science Foundation Grant MCB-8996274 (L.C.M.) and National Science Foundation Plant Biology Postdoctoral Fellowship DIR-9104365 (J.D.H.). Additional support was provided by a D. J. Sibley Centennial Fellowship in Plant Molecular Genetics (L.C.M.), a grant from the University Research Institute at the University of Texas (L.C.M.), a Bess Heflin Graduate Fellowship (C.L.B.), and an NSF REU Fellowship (J.V.M.).

* Author to whom correspondence should be addressed.

[1] Abbreviations: PIPES, piperazine-*N*,*N*′-bis(2-ethanesulfonic acid) dipotassium salt; EGTA, ethylene glycol bis(β-aminoethyl ether)-*N*,*N*,*N*′,*N*′-tetraacetic acid; IB, isolation buffer (50 mM PIPES–KOH, pH 6.9, 1 mM EGTA, 0.5 mM $MgSO_4$, and 1 mM DTT); GTP, guanosine 5′-triphosphate (trilithium salt); DMSO, dimethyl sulfoxide; MAPs, microtubule-associated proteins.

0006-2960/93/0432-3437$04.00/0

In fact, the few existing studies on plant tubulin indicate that it has pharmacological properties which are distinct from those of mammalian tubulin [reviewed in Morejohn (1991)]. Plant microtubules are commonly resistant to anti-microtubule compounds derived from plant secondary metabolism, such as colchicine (Levan, 1954; Morejohn & Fosket, 1984a) and vinblastine (Segawa et al., 1981), and are sensitive to different chemical classes of synthetic herbicides which have no effect on mammalian microtubules (Morejohn & Fosket, 1984b; Morejohn et al., 1987a).

Taxol does not interact identically with microtubules from a variety of nonanimal cells. For example, taxol neither induces the polymerization of tubulin nor stabilizes preformed microtubules purified from the budding yeast *Saccharomyces cerevisiae* (Barnes et al., 1992). Certain related taxane alkaloids do not effectively stabilize microtubules from the slime mold *Physarum polycephalum* against depolymerization by treatment with low temperature (4 °C) (Lataste et al., 1984). Early studies on the assembly of plant tubulin (Morejohn & Fosket, 1982, 1984a) demonstrated that taxol induces the polymerization of rose microtubules more effectively than glycerol, but that the taxol-induced polymerization reaction is much weaker than taxol-induced mammalian tubulin assembly (Kumar, 1981). Specifically, in the presence of 1 M sucrose, a tubulin-stabilizing component (Frigon & Lee, 1972), and assembly-saturating concentrations of taxol, the rates of plant tubulin assembly are relatively slow, showing sigmoidal turbidity kinetics, rather than the hyperbolic kinetics exhibited by bovine brain tubulin. Under these conditions short plant microtubules are formed, and only 56–58% of plant tubulin polymerizes in the presence of taxol, whereas ≥75% of bovine brain tubulin polymerizes under identical conditions (Morejohn & Fosket, 1984a). The relatively weak polymerization characteristics of plant tubulin point to the possibilities that (i) plant microtubules have an intrinsically lower affinity for taxol than do animal microtubules, (ii) isolated plant tubulin has an inherently lower competence to polymerize, and /or (iii) the buffer composition or conditions of assembly were suboptimal for polymerization. In addition, it is not known whether taxol stabilizes plant microtubules in vitro against the depolymerizing effects of low temperature or Ca^{2+}. Thus, neither the taxol-induced assembly characteristics of plant tubulin nor the potential of taxol for use in plant microtubule biochemistry has been explored adequately.

In the present work we have examined in detail the taxol-induced polymerization of plant tubulins isolated by a streamlined method which provides milligram quantities of assembly-competent tubulin from suspension cultures of maize (*Zea mays* cv. Black Mexican Sweet; BMS) and tobacco (*Nicotiana tabacum* cv. Bright Yellow 2; BY-2). These model cell lines were chosen because of their well-characterized microtubule cytoskeletons [e.g., Wang et al. (1989) and Hasezawa et al. (1991)]. Preliminary studies showed that sucrose inhibits the rate and extent of taxol-induced plant tubulin polymerization (L. C. Morejohn, unpublished results), and for this reason, all subsequent experiments were performed in the absence of sucrose. Our experiments establish for the first time that low concentrations of taxol induce the polymerization of ≥95% of isolated plant tubulin dimer. The estimated values of C_c for BMS tubulin (0.06 mg/mL) and BY-2 tubulin (0.13 mg/mL) are substantially lower than that previously reported for the taxol-induced assembly of rose tubulin (0.21 mg/mL) (Morejohn & Fosket, 1984a) and of bovine brain tubulin (0.3–0.4 mg/mL) (Kumar, 1981). However, in the absence of sucrose, taxol promotes the assembly of plant tubulin into many aberrant polymorphic structures, such as sheets and ribbons, in addition to microtubules. The control of polymerization initiation events, either by gradual temperature ramping or by inclusion of the anti-microtubule herbicide oryzalin (Morejohn et al., 1987a), slows the rate of taxol-induced plant tubulin polymerization, minimizes the formation of polymorphic polymers, and produces morphologically normal microtubules. Interestingly, both the rate and extent of plant tubulin polymerization at low temperature are much greater than those of bovine brain tubulin, probably reflecting a novel functional difference between the polymerization domains of these diverse tubulins. Taxol-stabilized plant microtubules may be purified to homogeneity by a single centrifugation step and are efficiently depolymerized by a combined treatment of cold and Ca^{2+}. Our findings provide the first evidence that plant tubulin may be subjected to numerous rounds of efficient and reversible taxol-induced tubulin assembly with little loss of polymerization competence.

MATERIALS AND METHODS

Materials. Taxol was generously provided by Dr. Nancita Lomax, Drug Synthesis and Chemistry Branch, Division of Cancer Treatment, National Cancer Institute, Bethesda, MD, and analytical grade (98.6%) oryzalin was obtained from Eli Lilly and Co., Indianapolis, IN. Stock solutions of 10 mM taxol and 1 mM oryzalin were prepared in DMSO and stored at −80 °C until use. Ultrapure ammonium sulfate was obtained from ICN (Irvine, CA), and Miracloth filter sheet and pectolyase were purchased from Calbiochem (La Jolla, CA). Electrophoresis chemicals, except SDS, were from Bio-Rad (Richmond, CA), and all other chemicals and chromatographic materials and cellulysin were obtained from Sigma Chemical Co. (St. Louis, MO).

Plant Cell Cultures. Liquid suspension cultures of maize BMS cells (*Z. mays* cv. Black Mexican Sweet) and tobacco BY-2 cells (*N. tabacum* cv. Bright Yellow 2) were grown in the dark at 28 °C and 145 rpm on an orbital shaker. Cells were grown in modified MS medium (Murashige & Skoog, 1962). For BMS cells, culture medium was supplemented with 150 mg/L L-asparagine, 2 mg/L 2,4-dichlorophenoxyacetic acid, 0.5 mg/L thiamine hydrochloride, and 20 g/L sucrose (pH 5.7), and for BY-2 cells, culture medium was supplemented with 100 mg/L myoinositol, 0.2 mg/L 2,4-dichlorophenoxyacetic acid, 1 mg/L thiamine hydrochloride, 255 mg/L KH_2PO_4, and 30 g/L sucrose (pH 5.8). Cells were subcultured at 7-day intervals by 10-fold dilution with fresh medium.

Tubulin Isolations. Plant tubulin was isolated from stationary-phase (day 7–8) cells (0.25–1.2 kg fresh weight) by DEAE-Sephadex A50 chromatography as described by Morejohn and Fosket (1982) with several modifications. Although the procedure provides milligram quantities of 80–90% pure plant tubulin (Morejohn et al., 1984), certain aspects of the procedure were reexamined to streamline the method and to improve the yield of tubulin for polymerization studies. Suspension cultures were used as a source of plant tubulin because large quantities (kilograms) of homogeneous cells may be grown quickly and inexpensively. Microtubules were depolymerized in vivo by low-temperature treatment (0 °C) of cultures prior to homogenization. The time-dependent depolymerization of microtubules in cells at 0 °C was assessed by performing indirect immunofluorescence microscopy (Simmonds et al., 1985) on samples fixed at different intervals. Virtually all microtubules in BMS cells are lost within 45 min

of cold treatment, but a small subpopulation of cold-stable microtubules persists for periods beyond 4 h. Microtubules in BY-2 cells are more resistant to cold treatment than those in BMS cells, yet most BY-2 microtubules are absent after 2 h of cold treatment. Residual cold-stable microtubules in BY-2 cells remain for periods greater than 4 h. On the basis of these pilot experiments all tubulin isolations were performed with cells chilled at 0 °C for a minimum of 2 h prior to homogenization.

Plant tubulin dimer is isolated typically from total cellular protein supernatants by step gradient elution of a DEAE-Sephadex A50 column: unbound proteins (fraction A) pass directly through, loosely bound proteins (fraction B) are eluted with 0.4 M KCl, and tubulin (fraction C) is eluted with 0.8 M KCl. Although this method produces 80–90% pure tubulin in fraction C (Morejohn et al., 1984), our previous immunoblotting experiments with a polyclonal antibody against plant α-tubulin showed some loss of tubulin to fraction B proteins when the DEAE column is washed with 0.4 M KCl prior to fraction C elution (Morejohn et al., 1985). Gel immunoblotting was used in preliminary experiments to optimize the elution protocol for an increased tubulin yield in fraction C. It was found that elution of fraction B with 0.35 M KCl provides a greater tubulin yield in fraction C, with an acceptable decrease in tubulin purity. These results are typical of tubulin isolations from both BMS and BY-2 cells, during which 40–80 μg of tubulin/g of cells (wet weight) is obtained. When 500–700 g of cells are processed, the entire procedure usually takes 8–9 h.

The following optimized protocol was used for all tubulin isolations in this study. Cells were combined in a 2-L flask containing medium and were chilled to 0–2 °C by continuous orbital shaking at 50 rpm in wet ice for 2–3 h in the dark. All subsequent operations were conducted at 4 °C. Cells were collected on a Miracloth filter, washed with ice-cold isolation buffer (IB) (1 mL/g of cells) consisting of 50 mM PIPES–KOH, pH 6.9, 1 mM EGTA, 0.5 mM $MgSO_4$, and 1 mM DTT, and supplemented with 10 mM diethyldithiocarbamic acid, 50 μg/mL TAME, and 5 μg/mL each of leupeptin, pepstatin, and aprotinin. Cells in batches of 200–330 g (wet weight) were homogenized for 5 min in the same buffer (0.25 mL/g wet weight) containing 1 mM GTP in an Omni-Mixer homogenizer at top speed. The homogenate was filtered through three biased layers of Miracloth, and the filtrate was centrifuged at 30000g for 1 h. The supernatant was swirled in the dark for 1 h in a flask containing DEAE-Sephadex A50 (0.25 mL of resin/mL of supernatant). The mixture was deaerated and poured into a glass chromatography column (2.5 × 40 cm or 5 × 20 cm), and unbound proteins (fraction A) were eluted directly at 18 mL/min and collected by precipitation with $(NH_4)_2SO_4$ at 90% saturation at 4 °C. Loosely bound proteins were eluted at 10 mL/min with 5 bed volumes of 0.35 M KCl–IB containing 0.1 mM GTP (fraction B) and were precipitated with $(NH_4)_2SO_4$ at 80% saturation. The tubulin-containing fraction (fraction C) was eluted with 3 bed volumes of 0.8 M KCl–IB containing 0.1 mM GTP and concentrated 35–60-fold by precipitation with $(NH_4)_2SO_4$ at 50% saturation. Protein fractions A and B were desalted on a Sephadex G10 column equilibrated with IB containing 0.1 mM GTP, 1 mM dithiothreitol, 50 μg/mL TAME, and 1 μg/mL each of leupeptin, pepstatin, and aprotinin. It was found that gel filtration and dialysis steps for removal of ammonium sulfate from tubulin (fraction C) precipitates (Morejohn et al., 1984) are unnecessary, because trace amounts of ammonium sulfate do not interfere with taxol-induced polymerization. Consequently, ammonium sulfate precipitates of fraction C tubulin were resuspended in the same buffer to approximately 4 mg/mL and used immediately or were frozen with liquid N_2 and stored at −80 °C. The yield of plant tubulin (40–80 μg/g fresh weight of cells) compares favorably with that (125 μg/g of brain tissue) obtained from calf brain by DEAE chromatography (Lee, 1982).

Brain tubulin was purified to ≥95% homogeneity from bovine brain cortex by DEAE-Sephadex A50 chromatography according to the method of Lee (1982), although the $MgCl_2$ precipitation step was omitted. The ammonium sulfate precipitate of tubulin was dissolved in IB containing 0.1 mM GTP, 1 mM dithiothreitol, and protease inhibitors, and samples were frozen and stored as above.

Gel Electrophoresis, Quantitative Densitometry, and Protein Determination. Proteins were analyzed by SDS–PAGE (8% polyacrylamide; 0.75-mm thickness) according to the method of Laemmli (1970). Gels were stained overnight in 0.125% Coomassie Brilliant Blue R-250 in 50% methanol–10% acetic acid, destained 1 h in 50% methanol–10% acetic acid, and further destained in 5% methanol–7% acetic acid. Estimations of tubulin purity in fraction C were made by quantitative densitometry of dried Coomassie-stained gels using an E-C densitometer equipped with a Hewlett-Packard integrator/plotter. Protein determinations were made with Bio-Rad protein dye reagent, and bovine serum albumin was used as a standard, with tubulin concentrations corrected by a factor of 2 as described previously (Morejohn et al., 1984). For calculations of tubulin concentration the molecular mass of tubulin was assumed to be 100 kDa on the basis of sequencing studies on plant tubulin genes (Fosket, 1989).

Turbidimetric Measurements and Polymer Sedimentation Assays. Microtubule assembly was monitored turbidimetrically by following the change in absorbency at 350 nm (ΔA_{350}) (Gaskin et al., 1974; Berne, 1974) using either a Beckman DU-60 spectrophotometer equipped with a Beckman Peltier temperature controller or a Perkin-Elmer Lambda 4C spectrophotometer equipped with a digital temperature controller accessory. Samples of plant tubulin (fraction C) or bovine brain tubulin were thawed in wet ice and clarified of insoluble material by centrifugation for 1 h at 100000g and 2 °C in a Beckman TL-100 ultracentrifuge (TLA-100.3 rotor). For polymerization experiments clarified tubulin samples were mixed with desired concentrations of taxol (final 1–2% DMSO in all reactions) in IB containing 0.1 mM GTP; each reaction mixture (250–350 μL) was immediately transferred to a quartz cuvette (0.7-mL volume, 1-cm light path), and the ΔA_{350} was recorded.

The mass of tubulin polymerized in each reaction was determined by polymer sedimentation assays (Johnson & Borisy, 1975). Polymer was sedimented by centrifugation through a 20% sucrose–IB cushion (40 μL) at 30000g for 30 min with a Beckman TL-100 ultracentrifuge (TLA-100 rotor).

Electron Microscopy. The ultrastructural morphology of plant tubulin polymers was studied with transmission electron microscopy as described by Kim et al. (1979), with the following modifications. Assembled polymer was sedimented through sucrose cushions as described above, and pellets were fixed overnight at room temperature in 1% glutaraldehyde–1% tannic acid in IB prepared with PIPES–NaOH (rather than PIPES–KOH), pH 6.9, and then post-fixed for 30 min at 4 °C with 0.5% osmium tetroxide in the same buffer. Pellets were embedded in 1% agarose, stained en bloc for 6 h with 1% uranyl acetate, and dehydrated through a graded ethanol series and propylene oxide. Pellets were embedded in EMbed-

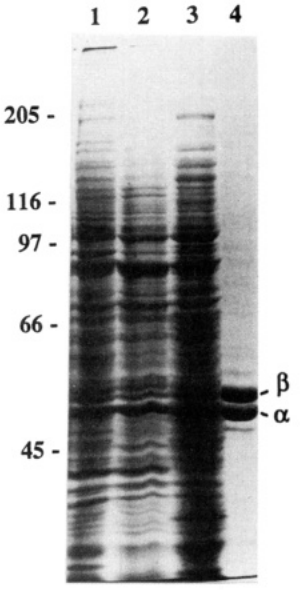

FIGURE 1: Isolation of BMS tubulin by DEAE-Sephadex A50 chromatography. SDS–PAGE analysis (Laemmli, 1970) shows Coomassie blue-stained polypeptides in ammonium sulfate precipitates of (1) whole-cell supernatant, (2) fraction A, (3) fraction B, and (4) fraction C. Lanes 1–3 contain approximately 80 μg of protein, and lane 4 contains 20 μg of protein. Positions of molecular weight marker proteins ($\times 10^3$) are indicated on the left, and positions of tubulin α- and β-subunits, which run in a reverse order in this gel system (Morejohn & Fosket, 1982; Cyr et al., 1987), are shown on the right.

812/Araldite and sectioned on an LKB Ultrotome ultramicrotome. Sections (50–60-nm thickness) were placed on EMS 300-mesh copper glider grids and stained for 30 min in 2% uranyl acetate in 12.5% methanol–35% ethanol and then for 3–5 min in Reynold's lead citrate. Electron microscopy was performed on a Jeol JEM-100CX electron microscope, and scoring of polymer morphology was accomplished with a dissecting microscope by direct observations of negatives illuminated with a light box.

Gel Filtration Chromatography. Taxol was chromatographically separated from tubulin dimer (0.5–1.5 mL) on a water-jacketed glass column (1 × 13 cm) packed with Sephadex G10 to provide a bed volume equal to 4–5 times the sample volume. The column was equilibrated with IB containing 0.1 mM GTP and was operated at 0 °C by continuous recirculation of ice–water through the jacket in a cold room (4 °C). The tubulin peak was collected in several 0.1-mL fractions, and each fraction was assayed for protein. To prevent contamination of protein by the leading shoulder of the taxol peak, the last 2–3 tubulin fractions eluted from the column were discarded. This results in a 70–80% recovery of tubulin from the column.

RESULTS

Polymerization Requirements of Plant Tubulin for Taxol. Detailed polymerization studies were performed with tubulin isolated from BMS cells, and when possible, these results were compared with data obtained in parallel studies with BY-2 tubulin. SDS–PAGE analysis of BMS cell protein fractions generated in a typical tubulin isolation is shown in Figure 1. Quantitative densitometry of BMS and BY-2 tubulins routinely affords 70–80% purity, and in this particular gel system (Laemmli, 1970) the tubulin α-subunit migrates faster than the β-subunit (Cyr et al., 1987).

Previous turbidimetric studies on the taxol-induced polymerization of rose tubulin showed a pronounced lag phase and a gradual rapid phase, which produced sigmoidal polymerization kinetics (Morejohn & Fosket, 1984; Morejohn et al., 1987b). This kinetic pattern indicated a relatively weak assembly process of plant tubulin. Our preliminary studies on solution components showed that sucrose (1 M), a tubulin-stabilizing agent (Frigon & Lee, 1972), transforms the hyperbolic turbidity kinetics of taxol-induced plant tubulin assembly into sigmoidal kinetics, which indicates a delay in polymer nucleation and elongation events (Oosawa & Asakura, 1975). Moreover, sucrose inhibited the extent of taxol-induced plant tubulin polymerization by 18% (L. C. Morejohn, unpublished results). For these reasons sucrose was omitted from the tubulin isolation procedure (see Materials and Methods) and from the assembly reaction buffer in the present work.

Quantification of the polymerization requirements of plant tubulin for taxol at 25 °C was made by polymer sedimentation analysis (Johnson & Borisy, 1975). Following 1 h of polymerization of 2.8 and 5.6 μM BMS tubulin (100-μL reaction volumes) with different concentrations of taxol (0.5–25 μM), polymer was sedimented by centrifugation, and pellets were assayed for protein. Figure 2A relates the yield of polymerized tubulin to the concentration of taxol used in the assembly reaction and shows that maximum polymerization is achieved with nearly 2:1 molar ratios of taxol and BMS tubulin. Parallel polymerization experiments with isolated BY-2 tubulin (6 and 10 μM) and different concentrations of taxol (0.25–25 μM) at 25 °C show maximum BY-2 polymer yield at nearly 2:1 molar ratios of taxol to tubulin (data not shown), indicating that tubulins from maize and tobacco have similar requirements for taxol. These experiments also show that in the presence of assembly-saturating concentrations of taxol ≥82% of soluble dimer is polymerization competent.

Low C_c for Taxol-Induced Plant Tubulin Polymerization. To obtain information on the C_c, the kinetics of BMS tubulin polymerization were observed turbidimetrically by monitoring the change in absorbence (A) at 350 nm (Gaskin et al., 1974). Different concentrations of tubulin (0.2–1 mg/mL) were polymerized with an assembly-saturating concentration of taxol (20 μM) in 215-μL reactions at 25 °C. Both the rate and the extent of turbidity development increase with increasing tubulin concentrations (Figure 2B, inset). Polymerization reactions with 0.4–1.0 mg/mL tubulin have hyperbolic turbidity kinetics composed of a rapid assembly phase, with apparent steady-state achieved within 15 min. Only the reaction containing a relatively low tubulin concentration (0.2 mg/mL) exhibits a lag phase and sigmoidal kinetics (Figure 2B, inset). Very similar results were obtained with BY-2 tubulin under the same assembly conditions, although higher absorbency values were observed. For example, taxol-induced polymerization of 0.6 mg/mL BY-2 tubulin produces a steady-state turbidity level (A_{350} = 0.6) which is nearly 5-fold greater than that (A_{350} = 0.125) produced by 1.0 mg/mL BMS tubulin.

To estimate the C_c for BMS tubulin, the initial BMS tubulin dimer concentration was plotted versus the extent of turbidity development, to provide C_c = 0.04 mg/mL at 25 °C (Figure 2B). Estimation of C_c using polymer sedimentation data derived from the same assembly experiments shows a similar slope and an estimated C_c = 0.06 mg/mL (Figure 2B). When the same polymerization analyses were performed with BY-2 tubulin, the turbidity method gave C_c = 0.08 mg/mL (correlation coefficient = 0.99), and the polymer sedimentation method afforded C_c = 0.13 mg/mL at 25 °C (correlation coefficient = 0.98) (data not shown). These estimated C_c

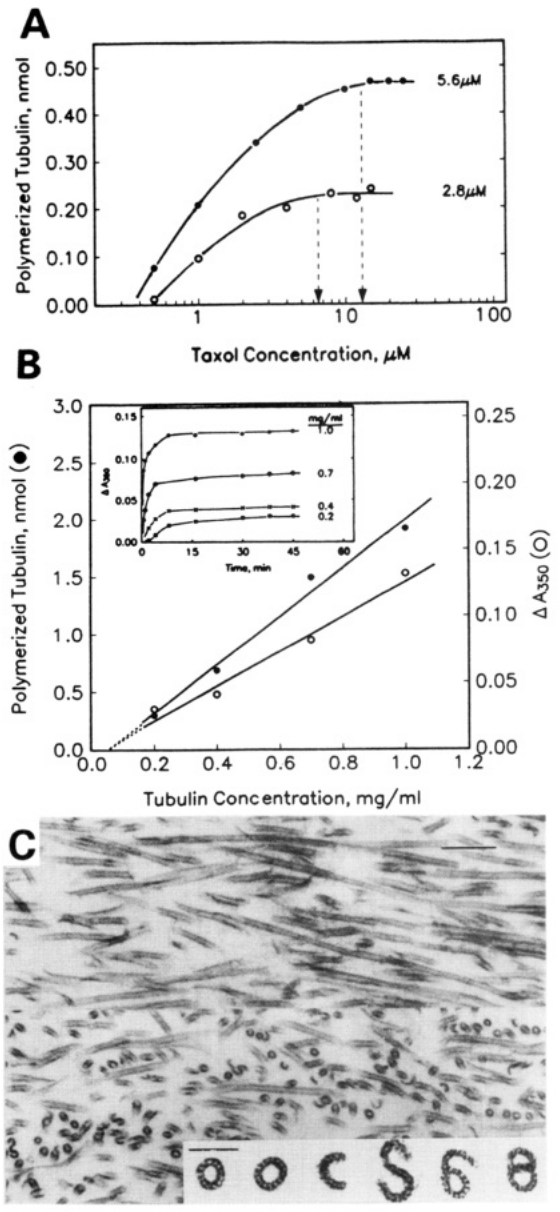

FIGURE 2: Analysis of taxol-induced BMS tubulin polymerization at 25 °C. (A) The dependence of polymerization on taxol concentration was examined with polymer sedimentation assays. BMS tubulin at 2.8 μM (○) and 5.6 μM (●) was polymerized for 1 h at 25 °C with different concentrations of taxol in a reaction volume of 100 μL, and polymer was sedimented by centrifugation at 30000*g*. The mass of sedimented polymer is expressed in nmol, and the estimated minimum concentration of taxol required for maximum polymer yield is designated with a dashed line and arrowhead for each tubulin concentration examined. (B) Estimation of the critical BMS tubulin dimer concentration (C_c) was made for taxol-induced polymerization. Inset: Different concentrations of tubulin were polymerized for 45 min at 25 °C with 20 μM taxol in a reaction volume of 215 μL, and polymerization kinetics were followed by turbidity development (ΔA_{350}). Tubulin concentrations are 0.2 (□), 0.4 (×), 0.7 (○), and 1.0 mg/mL (●). The amount of polymer (nmol) formed in each reaction was determined by sedimentation assay and is expressed as a function of the initial tubulin concentration. The extrapolated abscissa intercept for polymer mass (●) is 0.06 mg/mL (correlation coefficient = 0.97), and for maximum turbidity (○), 0.04 mg/mL (correlation coefficient = 0.97). (C) Electron micrographs of a thin-sectioned pellet show taxol-induced polymers formed from 1 mg/mL BMS tubulin at 25 °C; polymers are seen in longitudinal (upper) and cross section (lower). Scale bar = 0.2 μm. Inset: Electron micrographs of most commonly observed taxol-induced BMS polymers in cross section. Micrographs from left to right show a 13-protofilament microtubule, a 15-protofilament microtubule, a C-polymer, an S-polymer, a 6-polymer, and an 8-polymer. Scale bar = 50 nm.

values for plant tubulins are 2–4-fold lower than that (0.3–0.4 mg/mL) obtained with purified bovine brain tubulin under similar solution conditions (Kumar, 1981). In the absence of taxol (1 mM GTP; 2% DMSO; 25 °C) electron microscopy and polymer sedimentation revealed that C_c = 0.8–0.9 mg/mL for purified BMS and BY-2 tubulins (data not shown). This shows that taxol reduces the C_c for BMS and BY-2 tubulins 8–10-fold.

Taxol-Induced Formation of Polymorphic Plant Tubulin Polymers. Transmission electron microscopy was used to examine the morphology of polymers formed by 1 mg/mL BMS tubulin and 20 μM taxol after 1 h at 25 °C. The micrographs in Figure 2C show that most polymers are long, smooth-walled microtubules, although many linear polymorphic structures are also formed. Scoring of polymer cross-sectional morphology (n = 1555) revealed 58% microtubules and 42% other linear polymorphic structures in this sample. Polymers are randomly oriented in the pellet, but sufficient numbers of transverse views exist to permit direct counts of the protofilament number in each polymer. Although most microtubules are composed of 13 protofilaments, some microtubules are composed of 14 or 15 protofilaments, and the most commonly observed polymorphic polymers have C-, S-, 6-, or 8-shaped cross sections. A gallery of micrographs illustrating these BMS tubulin polymers is given in the inset of Figure 2C. Electron microscopy of negatively stained preparations showed that many of the BMS tubulin polymers are apparently normal microtubules which open to form ribbons or sheets and that the BY-2 polymers are composed mainly of free protofilaments, protofilament sheets, and ribbons, with relatively few microtubules (data not shown). The polymorphic nature of BY-2 polymers probably produces the unusually high turbidity values noted above, because polymorphic structures are known to scatter more light than microtubules (Hamel et al., 1981; Waxman et al., 1981).

Although taxol has been shown to induce the formation of polymorphic brain tubulin structures (Schiff et al., 1979; Hamel et al., 1981; Thompson et al., 1981), conditions which might modulate polymerization to produce polymers having normal lattice structure have not been adequately explored. The fast early kinetics of turbidity development and electron microscopy observations suggested that polymorphic structures are produced by rapidly forming, aberrant oligomeric nuclei and/or by inappropriate polymer elongation events (Asakura & Oosawa, 1975). To test this idea, BMS tubulin was polymerized under conditions expected to limit microtubule nucleation and elongation rates, including a substoichiometric concentration of oryzalin, an herbicide inhibitor of assembly (Morejohn et al., 1987a), or low temperature (Thompson et al., 1981). BMS tubulin (0.5 mg/mL) was polymerized with taxol (10 μM) for 18 h either with 1 μM oryzalin at 25 °C or without oryzalin at 4 °C, and sedimented polymer pellets were processed for electron microscopy and assayed for protein. At 25 °C in the presence of oryzalin 65% of tubulin assembles into polymers (n = 577) which are 76% microtubules and 24% polymorphic structures. At 4 °C in the absence of oryzalin 82% of tubulin assembles; 83% of polymers (n = 1159) are microtubules, and 17% are polymorphic structures (data not shown). These results show that low temperature not only is more effective than oryzalin for suppression of abnormal taxol-induced polymerization events but also permits more tubulin polymerization. Because the extended period of assembly (18 h) was considered impractical for use in routine biochemical applications, the effects of low temperature were

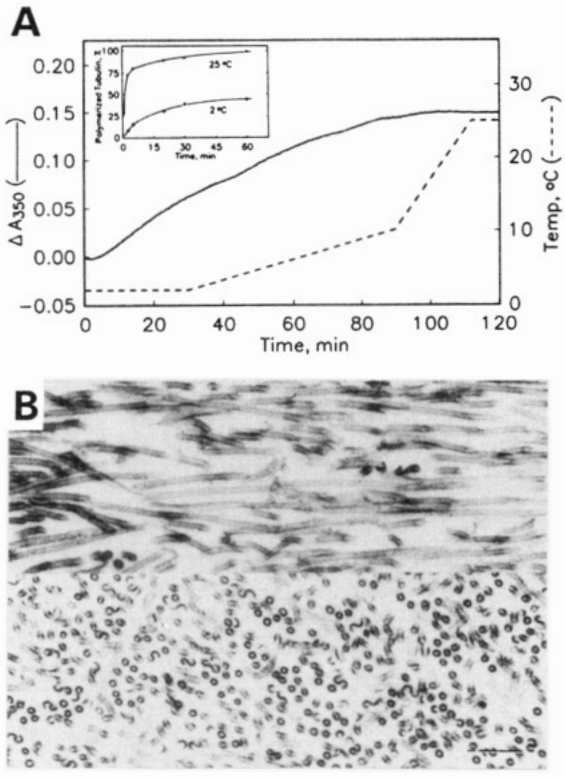

FIGURE 3: Effects of temperature on taxol-induced polymerization. (A) The kinetics of polymerization of tubulin (1 mg/mL) induced by taxol (20 μM) was recorded turbidimetrically (ΔA_{350}) during temperature ramping over 2 h. The solid and dashed lines represent the continuous change in turbidity (ΔA_{350}) and temperature, respectively. Inset: Polymer yields at 2 (●) and 25 °C (○) over 1 h were compared by sedimentation assays. The amount of polymer formed at each time point is expressed as the percent of soluble tubulin at time 0. (B) Electron micrographs of a thin-sectioned MT pellet show taxol-induced polymers formed after 2 h of ramped-temperature assembly; polymers are seen in longitudinal (upper) and cross section (lower). Scale bar = 0.2 μm.

investigated further in short-term, taxol-induced assembly reactions.

Polymerization of BMS tubulin (1 mg/mL) with taxol (20 μM) for 1 h at low temperature (2 °C) was examined by electron microscopy and polymer sedimentation analysis. Scoring of polymer cross sections (n = 650) in electron micrographs revealed 80% microtubules and 20% polymorphic structures (data not shown). Sedimentation analysis showed that substantial polymerization occurs within the first 30 min at 2 °C, but that only 48% of BMS tubulin polymerizes after 60 min at 2 °C compared to >95% polymerization at 25 °C (Figure 3A, inset). Apparently, short-term, low-temperature assembly conditions favor an ordered set of reactions which produces a high fraction of normal polymers. Such conditions unfortunately also create a higher C_c, which limits polymerization of most BMS tubulin dimer. These observations suggested that a gradual increase in temperature during tubulin assembly may facilitate a higher yield of normal polymer, a possibility which was explored.

Control of Taxol-Induced Plant Microtubule Polymerization by Low-Temperature Ramping. Various temperature ramping schedules were examined, and an optimized 2-h protocol having four steps was ultimately devised. The turbidimetric measurements shown in Figure 3A represent the temperature-regulated polymerization of 1 mg/mL BMS tubulin with 20 μM taxol. In this protocol the temperature is held for 30 min at 2 °C, increased 0.13 °C/min for 60 min to 10 °C and 0.75 °C/min for 20 min to 25 °C, and held for

Table I: Effect of Assembly Conditions on Morphology and Yield of BMS Polymer

reaction temp (°C)	polymerization time (h)	% microtubules in polymers (n)	% tubulin polymerized
25[a]	1	58 (1555)	≥82
2	1	80 (650)	48
25[b]	18	76 (577)	65
4	18	83 (1159)	82
2–25[c]	2	86 (1005)	≥95

[a] Temperature jumped from 0 to 25 °C. [b] Temperature jumped from 0 to 25 °C in the presence of 1 μM oryzalin. [c] Temperature ramped from 2 to 25 °C.

10 min at 25 °C. This ramping schedule produces turbidity measurements with sigmoidal kinetics composed of an obvious 3-min lag phase, a protracted rapid phase, and a 15–20-min steady-state period (final A_{350} = 0.15). These kinetics are noticeably different from those obtained when assembly is initiated with a temperature jump from 0 to 25 °C (compare with Figure 2B inset) and show that substantial BMS microtubule polymerization occurs at relatively low temperatures. Much of the tubulin assembles during the early 2 °C step (A_{350} = 0.06); half-maximal polymerization (A_{350} = 0.075) is achieved within 40 min as the temperature reaches 4 °C, and 95% of polymerization occurs within 90 min, as the temperature reaches 10 °C (Figure 3A).

Polymer sedimentation analysis showed that the ramping method does not increase the critical concentration, because virtually all the tubulin is polymerized. Electron microscopy analysis of sedimented polymers (n = 1005) demonstrated that more microtubules (86%) and fewer polymorphic structures (14%) are formed (Figure 3B) than with a rapid temperature shift. Longitudinal views of polymers did reveal that some individual microtubules are zippered open to form a protofilamentous sheet, either within a central region or at the end of the polymer, but temperature ramping minimizes this effect. Negative-stain electron microscopy observations indicated that the same ramping procedure efficiently assembles mostly normal appearing BY-2 microtubules (data not shown). These results intimate that low temperature controls the fidelity of nucleation events during taxol-induced plant tubulin polymerization and that temperature ramping generates plant microtubules in high yield. Because BY-2 polymers were visualized by negative-stain electron microscopy and BMS polymers were embedded and thin-sectioned, we were not able to make quantitative comparisons of polymorphic polymers formed by these two tubulins. A summary of the results of the electron microscopic and sedimentation analyses of BMS polymers formed under different polymerization conditions is displayed in Table I.

The results with plant tubulins were compared with those obtained with bovine brain tubulin also purified by DEAE-Sephadex chromatography (Lee, 1982). Much lower levels of brain tubulin polymerization were observed at low temperature than of plant tubulin. For example, when 0.6 mg/mL brain tubulin is assembled with 25 μM taxol (in IB containing 1 mM GTP) using the same 2-h temperature ramping schedule described above, turbidity measurements show little polymerization until the reaction temperature approaches 25 °C (110 min). When the sample is ramped subsequently from 25 to 37 °C at a rate of 1.2 °C/min and held constant at 37 °C, turbidity kinetics are sigmoidal, and maximum absorbency (A_{350} = 0.1) is achieved within 30 min. When a higher concentration of brain tubulin (1.5 mg/mL) is polymerized with taxol (20 μM) by ramping from 4 to 20 °C at 1.3 °C/min and then from 20 to 30 °C at 0.12 °C/min

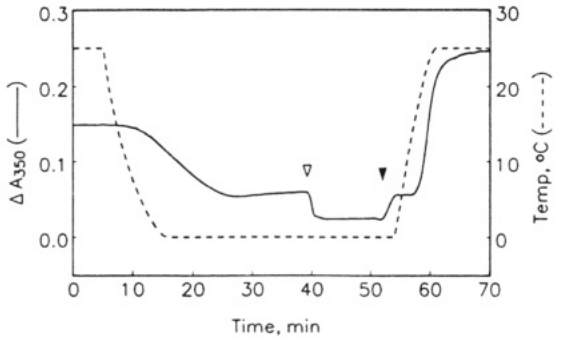

FIGURE 4: Reversible effects of low temperature and calcium on taxol-stabilized polymer. Taxol-stabilized BMS microtubules (1 mg/mL) previously polymerized with temperature ramping were treated sequentially with low temperature (0 °C), $CaCl_2$ (3 mM), EGTA (5 mM), and warm temperature (25 °C), and the continuous changes in absorbency (ΔA_{350}) (solid line) and temperature (dashed line) were recorded. The open and closed arrowheads indicate addition of 3 mM $CaCl_2$ and 5 mM EGTA, respectively.

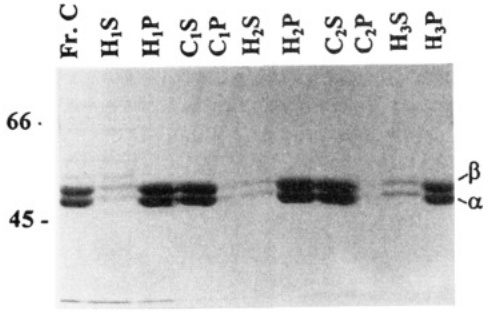

FIGURE 5: Cyclic BMS microtubule polymerization and depolymerization. Protein fractions from three cycles of reversible taxol-induced polymerization were separated by SDS–PAGE (Laemmli, 1970) and stained with Coomassie blue. Protein fractions are DEAE-isolated tubulin in fraction C (Fr. C), in heated supernatant (H_xS) and pellet (H_xP), and in chilled supernatant (C_xS) and pellet (C_xP) for each round, where subscript x = cycle number. On the left are positions of molecular weight markers (kDa), and on the right are positions of tubulin α- and β-subunits, which run in a reverse order in this gel system.

(total of 86 min), a turbidity increase is initiated at 20 °C, and turbidity kinetics are sigmoidal (maximum $A_{350} = 0.19$). Electron micrographs of negatively stained samples show abundant, long microtubules and very few polymorphic structures formed during temperature ramping (data not shown). Cumulatively these results demonstrate that at low temperature taxol induces the polymerization of plant tubulin much more rapidly than that of mammalian tubulin.

Reversible Effects of Low Temperature and Ca^{2+} on Taxol-Stabilized Plant Microtubules. The depolymerizing effects of low temperature and Ca^{2+} on taxol-stabilized microtubules were studied by turbidimetry and sedimentation analysis. BMS microtubules (1 mg/mL) previously assembled by temperature ramping with 20 μM taxol were treated initially with a temperature drop from 25 to 0 °C. Turbidity kinetics show that taxol-stabilized microtubules having an initial A_{350} = 0.15 begin to depolymerize as the temperature reaches 8 °C and continue gradual depolymerization for 17 min, at which time a new, low steady state ($A_{350} = 0.06$) is achieved (Figure 4). Upon addition of 3 mM $CaCl_2$ to the 0 °C reaction (open arrowhead) remaining cold-stable microtubules rapidly depolymerize within 1 min, and a lower steady-state level (A_{350} = 0.025) is obtained. Sedimentation analysis of parallel samples at this stage showed that microtubules are completely disassembled and that residual absorbancy is caused by small oligomeric forms of tubulin. Separate experiments also showed that when taxol-stabilized microtubules at 25 °C are resuspended by vigorous mixing with a pipette tip directly in Ca^{2+} buffer at 0 °C, depolymerization kinetics are so rapid that disassembly can not be measured spectrophotometrically. Under these conditions virtually all polymer is depolymerized within 2–5 min. However, efficient depolymerization depends also upon the initial concentration of taxol-stabilized polymer, because the rate and extent of depolymerization were found to decrease as the initial concentration of microtubules is increased. Similar results are obtained when taxol-stabilized BY-2 microtubules are depolymerized with combined cold and Ca^{2+}. For example, with BY-2 tubulin 67% of 2.8 mg/mL microtubules depolymerize, whereas 82% of 1.7 mg/mL microtubules depolymerize. In general, complete depolymerization of plant microtubules is obtained when the initial microtubule concentration is less than 1.5 mg/mL. Although 0.1–1 mM GTP was included in the depolymerization steps, the extent of microtubule depolymerization was found not to require the addition of GTP.

The ability of depolymerized BMS tubulin to directly repolymerize was also tested (Figure 4). Chelation of Ca^{2+} by addition of 5 mM EGTA (Figure 4, closed arrowhead) stimulates a small amount of repolymerization of 0 °C. When the reaction temperature is rapidly ramped from 0 to 25 °C, tubulin repolymerization is reinitiated around 15 °C, and rapid repolymerization continues for nearly 12 min. In this particular experiment the final steady-state turbidity value ($A_{350} = 0.25$) at 25 °C is substantially higher than the initial value ($A_{350} = 0.15$), because the rapid temperature increase during repolymerization produces polymorphic structures which scatter more light than microtubules (Hamel et al., 1981; Waxman et al., 1981). Alternatively, depolymerized tubulin may be efficiently repolymerized into normal microtubules after Ca^{2+} chelation by using the gradual ramping protocol described above (Figure 3).

These experiments demonstrate that plant tubulin can be efficiently polymerized with taxol and that taxol-stabilized plant microtubules are readily depolymerized by cold and Ca^{2+} treatment such that virtually all tubulin is efficiently interconverted between dimer and polymer. These characteristics of reversible polymerization are generally similar to those observed with mammalian tubulin (Hamel et al., 1981; Collins & Vallee, 1987) and prompted our examination of cyclic plant microtubule polymerization and depolymerization.

Cyclic Plant Microtubule Polymerization and Depolymerization. BMS tubulin (1 mg/mL) in fraction C was subjected to three successive cycles of polymerization and sedimentation, and the fractions generated were analyzed by Coomassie blue-stain SDS–PAGE (Figure 5). The amount of tubulin in gel lanes reflects the efficiency of the polymerization and depolymerization steps, because samples of each pellet were resuspended to an equivalent of the assembly volume, and corresponding supernatant and pellet samples were loaded at equal volumes. After polymerization at 25 °C and centrifugation through a 20% sucrose–IB cushion at 30000g for 30 min, the first heated supernatant (H_1S) has virtually no tubulin remaining, and most of the tubulin is concentrated in the first heated pellet (H_1P). The H_1P was resuspended to 80% of the original reaction volume in cold IB containing 3 mM $CaCl_2$; microtubules were depolymerized for 30 min on wet ice, and the sample was centrifuged at 30000g for 30 min at 2 °C. Figure 5 shows that the first chilled supernatant (C_1S) contains most of the tubulin, whereas very little cold-stable polymer exists in the first chilled pellet (C_1P). Repolymerization of C_1S tubulin was accomplished by addition of 5 mM EGTA and warming to 25 °C. Continued

cycles of polymerization and depolymerization were performed with a remarkably high cycling efficiency, indicating little loss of tubulin assembly competence (Figure 5). Essentially the same results are obtained with tubulin assembled with the gradual temperature ramping rather than with a temperature jump. Electron microscopy of cycled polymers showed an approximately 11% increase in the proportion of polymorphic structures at each 25 °C polymerization step, indicating that tubulin undergoes a very gradual denaturation during the procedure. It is important to note that silver-stained gels of this experiment showed H_1P tubulin to be electrophoretically pure, a result demonstrating that none of the polypeptides coisolated with tubulin in fraction C by DEAE-chromatography binds to microtubules like typical fibrous MAPs (data not shown).

Dissociation of Taxol from Plant Tubulin Dimer. Although reversible taxol-induced microtubule polymerization is an effective method for purification of tubulin from other fraction C proteins, the use of plant tubulin in applications such as MAP-induced microtubule polymerization studies or antimicrotubule drug binding experiments also requires prior separation of taxol from dimer. Previous studies with [^{3}H]-taxol and mammalian tubulin have shown that taxol binds to polymer, but not to the soluble tubulin dimer (Parness & Horwitz, 1981; Takoudju et al., 1988), and that taxol can be separated from tubulin dimer by gel filtration chromatography (Collins & Vallee, 1987). The possibility that taxol could be separated from BMS tubulin (C_1S) by gel filtration was initially explored by chromatography on a Sephadex G10 column equilibrated with IB containing 3 mM $CaCl_2$ at 0 °C. The rationale for inclusion of Ca^{2+} was that taxol-induced polymerization of BMS tubulin at low temperature would be inhibited during the chromatography procedure. This approach did not prove useful, however, because tubulin bound to the Sephadex resin and could not be eluted quantitatively with EGTA. Apparently, the binding of Ca^{2+} to BMS tubulin dimer exposes a hydrophobic domain(s) which interacts strongly with Sephadex. Separation of taxol from tubulin was reexamined with a Sephadex G10 column equilibrated at 0 °C with IB alone, and it was found that tubulin elutes from the column as expected, immediately following the void volume.

Polymerization of chromatographed C_1S tubulin (0.3 mg/mL) was monitored turbidimetrically at 25 °C in the presence or absence of 3 μM oryzalin. The results show that no tubulin polymerizes within the first 60 min, indicating efficient chromatographic removal of taxol from tubulin, and that, upon addition of a stoichiometric concentration (3 μM) of taxol, C_1S tubulin rapidly repolymerizes (Figure 6). Incubation of chromatographed tubulin with oryzalin for 60 min produces a small decrease in turbidity, probably resulting from the dissociation of small oligomeric forms of tubulin, and addition of 3 μM taxol does not overcome the inhibitory effect of oryzalin (Figure 6). These experiments indicate that taxol can be effectively separated from plant tubulin dimer by gel filtration chromatography essentially as has been shown for animal tubulin (Collins & Vallee, 1987). Confirmation of the removal of taxol may be made by HPLC analysis (Collins & Vallee, 1987). The results show that purified plant tubulin retains not only its ability to polymerize but also its characteristic herbicide-binding properties (Morejohn et al., 1987a).

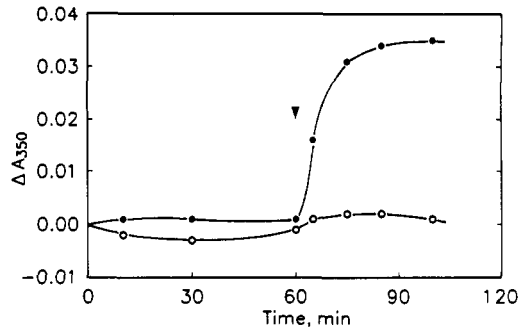

FIGURE 6: Separation of taxol from BMS tubulin dimer at low temperature. EGTA (5 mM) was added to chelate calcium in the taxol-containing C_1S fraction of BMS tubulin (3 μM), and the sample was subjected to Sephadex G10 chromatography in an ice–water-jacketed column to remove taxol. Chromatographed tubulin was incubated at 25 °C in the presence (○) or absence (●) of 3 μM oryzalin. Polymerization was monitored by recording the change in turbidity (ΔA_{350}) at the intervals shown. The arrowhead indicates addition of taxol to each sample at a final concentration of 3 μM.

DISCUSSION

Most animal cells possess extensive microtubule cytoskeletons, and some organs such as brain are disproportionately rich in tubulin and MAPs by comparison to plant tissues. Consequently, animal microtubule proteins may be readily isolated by direct polymerization of endogenous tubulin in crude cellular supernatants. Application of this method to crude plant supernatants has met with limited success because plant tissues are not particularly rich in microtubule proteins and may possess factors which inhibit microtubule polymerization (Morejohn & Fosket, 1986). Nevertheless, tubulin may be isolated from cultured higher plant cells by ion-exchange chromatography and subsequently polymerized into microtubules (Morejohn & Fosket, 1982). Because plant cells can be grown very rapidly as suspension cultures in inexpensive defined media, several hundred grams of cells may be obtained in only a few days. We have demonstrated in the present study that assembly-competent plant tubulin can be readily isolated from cultured cells with reasonable purity and in relatively high yield.

Previous studies on taxol-induced plant tubulin assembly showed sigmoidal turbidity kinetics when assembly was initiated with a rapid temperature jump (Morejohn & Fosket, 1984a; Morejohn et al., 1987b), rather than the hyperbolic kinetics which we observed herein. In these early studies the effects of colchicine on taxol-induced polymerization was also examined, and because sucrose prevents the decay of the colchicine-binding site and stabilizes dimeric tubulin (Frigon & Lee, 1972), 1 M sucrose was included in the assembly buffer. In the current work sucrose was omitted from the tubulin isolation procedure (see Materials and Methods) and from the assembly buffer because our preliminary experiments showed that sucrose partially inhibits taxol-induced plant tubulin assembly (L. C. Morejohn, unpublished results). An inhibitory effect of sucrose on polymerization has been reported also for porcine brain tubulin (Barton, 1978), and more recent X-ray diffraction studies of calf brain microtubules have confirmed that sucrose alters the conformational state of tubulin in microtubules (Beese et al., 1987). The inhibitory effects of sucrose on polymerization may also result from an increase in solution viscosity, which produces decreased diffusion rates of dimer and polymer. Another notable difference between the previous and present results is that only 56–58% of rose tubulin was shown to polymerize (Morejohn & Fosket, 1984a), while ≥95% of plant tubulin dimer assembled in the current study. We speculate that the previously used step of overnight dialysis of tubulin to remove ammonium sulfate may have resulted in some decay of the dimer and a loss of assembly competence. This step has been

omitted from the isolation procedure, and we now obtain plant tubulin having excellent assembly competence. The quality of our plant tubulin preparations is revealed by the very low estimated C_c for maize tubulin (0.06 mg/mL) and tobacco tubulin (0.13 mg/mL) when polymerized with taxol at 25 °C. Indeed, these values are 2–4-fold lower than that (C_c = 0.3–0.4 mg/mL) reported for purified bovine brain tubulin at 37 °C (Kumar, 1981) and approach the concentration (0.02 mg/mL) at which mammalian dimers dissociate into monomers at 5 °C (Sackett & Lippoldt, 1991).

Maximum BMS and BY-2 microtubule polymerization is achieved at a 2:1 molar ratio of taxol to tubulin, which is different from that observed for the assembly of bovine brain microtubules (Kumar, 1981; Parness & Horwitz, 1981). These differences may reflect different numbers of taxol-binding sites on these diverse plant tubulins. A more likely explanation is that plant tubulins have a somewhat lower affinity for taxol than does mammalian tubulin, and they require higher taxol concentrations to drive the assembly reaction.

Microtubules are known to self-assemble in a two-phase manner (Oosawa & Asakura, 1974). The first phase, nucleation, involves the transient association and dissociation of dimers until critical oligomeric nuclei are formed. The second phase of microtubule polymerization involves the elongation of these nuclei by the head-to-tail interactions of dimers to form protofilaments, which become laterally associated to form the cylindrical, 13-protofilament microtubule structure. The protofilament number in microtubules assembled in vitro can be controlled by the manipulation of assembly buffer constituents, ionic strength, and pH (Bohm et al., 1984). The molecular mechanism by which taxol promotes tubulin polymerization is not yet fully understood, but polymerization experiments suggest that the nucleation phase of assembly is strongly enhanced. It has been suggested that taxol stabilizes dimer–dimer interactions and shifts the assembly reaction equilibrium toward polymerization (Parness & Horwitz, 1981; Manfredi & Horwitz, 1984). When plant tubulin dimer is assembled with taxol using a rapid temperature jump (0–25 °C), polymers consist of a large number of polymorphic structures, which may result from aberrant dimer associations during the nucleation phase of polymerization. In the absence of taxol, abnormal nuclei may form as well, but these are unstable and dissociate, whereas taxol may stabilize a variety of different nuclei, some of which are aberrant and become elongated into a number of polymorphic structures. Previous observations that short microtubules and few polymorphic structures are formed by plant tubulin in the presence of 1 M sucrose (Morejohn & Fosket, 1984a) suggest that, under conditions of high viscosity, polymerization events are more ordered, presumably due to concomitantly lower molecular diffusion rates. This notion is supported also by our current observations that a higher fraction of normal plant microtubules is formed when nucleation is limited either by low temperature (2 °C) or by inclusion of the anti-microtubule herbicide oryzalin at 25 °C. Although we found that the yield of taxol-induced plant microtubules is reduced at low temperature, temperature ramping (2–25 °C) permits high-fidelity nucleation events to occur early during assembly and provides relatively few polymorphic structures and a high yield of polymer. Previously reported polymorphic structures formed by plant tubulin in the presence of sucrose were shown to result from proteolytic clipping of the dimer during its isolation, a problem which may be avoided with the use of certain protease inhibitors (Morejohn et al., 1985). Polymorphic structures observed in this study did not result from proteolysis, because tubulin was prepared with buffer containing a cocktail of protease inhibitors, and neither SDS–PAGE nor immunoblotting with anti-tubulin antibodies revealed evidence of tubulin subunit proteolysis.

Taxol binds to a single set of high-affinity binding sites on mammalian brain tubulin, having a K_d = 0.87 μM (Parness & Horwitz, 1981). The similar assembly-promoting and stabilization effects of taxol which we have found on tubulins from plants and animals suggest that taxol binds with high affinity to polymerized tubulins from both groups of organisms. This result is somewhat surprising in view of the fact that other anti-microtubule compounds have very different affinities for these diverse proteins. For instance, the microtubule depolymerizing drug colchicine, an alkaloid from the higher plant genus *Colchicum*, binds to rose tubulin with a much lower affinity ($K_a = 9.7 \times 10^2\ M^{-1}$) than to mammalian tubulin ($K_a = 2.6 \times 10^6\ M^{-1}$) (Morejohn et al., 1987b). The synthetically derived herbicides oryzalin and amiprophos-methyl inhibit polymerization of plant tubulin at low micromolar concentrations, but have no effect on the assembly of bovine brain tubulin (Morejohn & Fosket, 1984b; Morejohn et al., 1987a). Previous studies have shown also that taxol and certain related taxane alkaloids do not interact identically with microtubules from diverse organisms. Neither taxol nor 10-acetylbaccatin III stabilizes purified microtubules from the budding yeast *Saccharomyces cerevisiae* against dilution-induced disassembly (Barnes et al., 1992). Although taxol and the taxane derivative 10-deacetylbaccatin III stabilize microtubules from the slime mold *Physarum polycephalum* against low-temperature-induced depolymerization, 10-deacetylbaccatin III does not effectively stabilize mammalian microtubules (Lataste et al., 1984). For these reasons we examined in detail the effects of taxol on plant tubulin assembly and polymer stability. Despite the fact that taxol is a plant secondary product, the results of this study show effects of taxol on plant microtubules which are remarkably similar to those reported for mammalian microtubules. Apparently, the taxol-binding site has been highly conserved since the divergence of primitive plant and animal cells from a common ancestral cell.

Direct photoaffinity labeling experiments have demonstrated that [^{3}H]taxol binds to the β-subunit of mammalian brain tubulin (Rao et al., 1992), so it is reasonable to speculate that the taxol-binding site(s) resides also on the plant β-subunit. This idea is consistent with the findings of a comparative analysis of the primary amino acid sequences of angiosperm and vertebrate tubulins wherein more nonconservative substitutions are found in α-subunits than in β-subunits (Fosket & Morejohn, 1992). Interestingly, several kingdom-specific, nonconservative substitutions were pinpointed within the polymerization domains of α-tubulin (Fosket & Morejohn, 1992), and some of these substitutions reside within putative intermolecular contact regions between adjacent structural domains (de la Vina et al., 1988). These α-tubulin substitutions may produce unique polymerization characteristics of the plant tubulin dimer, and we speculate that rapid assembly of plant microtubules at low temperature is a manifestation of a functional difference in the polymerization domains of plant and mammalian tubulins, rather than a difference in their taxol-binding sites.

The observation that taxol induces plant tubulin to form a variety of polymorphic structures when the temperature is rapidly jumped from 0 to 25 °C is consistent with previous reports on polymorphic structures formed by pure mammalian tubulin and taxol (Schiff et al., 1979; Hamel et al., 1981;

Bohm et al., 1984). Polymorphic polymers are of potential concern for future plant MAP studies, because it is not known whether plant MAPs bind with high fidelity to polymorphic tubulin structures such as sheets, ribbons, or free protofilaments. Direct support for this notion comes from recent work demonstrating that extremely different lattice structures of mammalian tubulin polymer dramatically affect kinesin-dependent motility (Kamimura & Mandelkow, 1992). Another potential concern was that tubulin domains which are normally confined within the microtubule lumen are exposed in polymorphic structures and may inappropriately bind components in the proteinaceous milieu which have no relationship to MAPs. Fortunately, we were able to develop a convenient and efficient procedure of temperature-ramped assembly, which provides a high yield of polymer and 86% normal appearing microtubules. Most of the taxol-assembled plant microtubules we observed in cross section are composed of 13 or 14 protofilaments, but these relatively minor lattice polymorphisms are expected to have little effect on MAP–microtubule interactions in vitro, because MAPs bind to microtubules having different numbers of protofilaments (Bohm et al., 1984).

Our findings that calcium causes the depolymerization of taxol-stabilized plant microtubules and that taxol may be separated from depolymerized tubulin dimer by gel filtration chromatography are in accord with previous mammalian tubulin studies (Collins & Vallee, 1987; Takoudju et al., 1988). However, our turbidimetric measurements of assembly at 25 °C were only sensitive enough to detect the presence of ≥ 0.5 μM taxol, so that confirmation of the complete removal of taxol from plant tubulin may require HPLC (Collins & Vallee, 1987). Moreover, our results provide the first direct evidence that plant microtubules are sensitive to calcium and indirectly demonstrate the existence of a calcium-binding site(s) on the plant tubulin dimer. Although the potential role of calcium in the regulation of microtubule function has not been elucidated, calcium inhibits the polymerization of mammalian brain microtubules (Berkowitz & Wolff, 1981), and a high-affinity, calcium-binding site ($K_d = 2.8$ μM) has been reported (Solomon, 1977) within the carboxyl-terminal region of animal tubulin which binds MAPs (Serrano et al., 1986).

The carboxyl-terminal regions of mammalian α- and β-tubulin are considered regulatory domains which bind certain MAPs, such as tau and MAP 2, through electrostatic interactions. The MAP-binding site consists of an internal constant subsite and an external acidic hypervariable subsite, also known as the isotype-defining region (Fosket & Morejohn, 1992). Studies on the acidic isotype region of mammalian β-tubulin have demonstrated its importance in the productive interaction with MAPs (Paschal et al., 1989) and that different isotypes bind MAPs differentially (Cross et al., 1991). These results suggest that differences between the external acidic subsite of isotypic tubulins may affect the affinity of MAP binding to microtubules. A comparison of the available carboxyl-terminal sequences of plant and vertebrate tubulins has revealed that the internal subsite is highly conserved over evolution, but that the external hypervariable subsites are too variable for direct comparisons (Fosket & Morejohn, 1992). Although the in vitro copolymerization of tubulin from diverse species (Yadav & Filner, 1983; Barnes et al., 1992) indicates a conservation of the polymerization domains of tubulin, there is no published evidence that the regulatory domains of plant and animal tubulins are conserved. In fact, we have obtained preliminary evidence that although bovine brain MAP 2 binds with normal stoichiometry to preformed, taxol-stabilized BMS microtubules, in the absence of taxol MAP 2 induces the polymerization of purified BMS tubulin into long polymorphic ribbon structures, rather than normal microtubules (Bokros et al., 1992). Control experiments show that in the absence of MAP 2 only long, normal BMS microtubules are formed (Bokros et al., 1992). These results suggest a subtle divergence of the MAP-binding regulatory domains on plant and mammalian tubulins and point to the a priori possibility that the use of mammalian brain microtubules to isolate heterologous MAPs may preferentially enrich only those MAPs having the most conserved microtubule-binding domains. For this reason the prudent investigator will use a homologous source of tubulin for plant MAP isolation studies, to ensure a high-fidelity interaction of plant MAPs with microtubules. To date, the isolation of putative higher plant MAPs by microtubule affinity has been reported in only four studies, all of which relied heavily or exclusively on the use of mammalian brain tubulin for the analyses (Cyr & Palewitz, 1989; Vantard et al., 1991; Tiezzi et al., 1992; Yasuhara et al., 1992). The results of the present study obviate the use of mammalian tubulin in plant studies, inasmuch as assembly-competent plant tubulin can be easily obtained in quantities sufficient to permit multiple rounds of microtubule polymerization and depolymerization.

A more comprehensive understanding of microtubule function during plant cell division and differentiation will come from further identifications of plant MAPs. Most animal MAPs have been identified by cyclic copolymerization with microtubules in cellular extracts. However, the relatively low tubulin concentrations in whole plant cell extracts present a major limitation to MAP isolation, because much tubulin is lost to the C_c, and the yield of microtubules is small even when using taxol-induced assembly (Vantard et al., 1991). In order to circumvent this problem, it should be possible first to isolate plant tubulin, to prepare taxol-stabilized microtubules, and to recombine the microtubules with MAP-containing fractions of plant proteins. As long as the concentration of microtubules after dilution is well above the C_c at each stage of polymerization, reversible taxol-induced assembly and MAP copolymerization should be feasible. Because taxol binding sites on mammalian brain microtubules are separate and distinct from MAP binding sites (Kumar, 1981; Vallee, 1982), taxol is unlikely to interfere with the binding of plant MAPs to microtubules. This approach to MAP identification is currently under investigation.

ACKNOWLEDGMENT

The authors thank Gordon Aalund for technical assistance, Ruben Mitchell (Cell Research Institute, University of Texas at Austin) for suggestions and assistance with electron microscopy, and Drs. R. Malcolm Brown, Jr. (University of Texas at Austin), and Donald E. Fosket (University of California at Irvine) in whose laboratories certain preliminary experiments were performed.

REFERENCES

Barnes, G., Louie, K. A., & Botstein, D. (1992) *Mol. Biol. Cell 3*, 29–47.

Barton, J. S. (1978) *Biochim. Biophys. Acta 532*, 155–160.

Beese, L., Stubbs, G., Thomas, J., & Cohen, C. (1987) *J. Mol. Biol. 196*, 575–580.

Berkowitz, S. A., & Wolff, J. (1981) *J. Biol. Chem. 256*, 11216–11223.

Berne, B. J. (1974) *J. Mol. Biol. 89*, 755–758.

Bohm, K. J., Vater, W., Femske, H., & Unger, E. (1984) *Biochim. Biophys. Acta 800*, 119–126.
Bokros, C. L., Hugdahl, J. D., Hanesworth, V. R., Aalund, G. R., & Morejohn, L. C. (1992) *Mol. Biol. Cell 3S*, 49a.
Burton, P. R. (1981) in *Cell and Muscle Motility* (Dowben, R. M., & Shay, J. W., Eds.) Vol. 1, pp 289–333, Plenum Press, New York.
Caplow, M., & Zeeburg, B.(1982) *Eur. J. Biochem. 127*, 319–324.
Collins, C. A., & Vallee, R. B. (1987) *J. Cell Biol. 105*, 2847–2854.
Cross, D., Dominguez, J., Maccioni, R. B., & Avila, J. (1991) *Biochemistry 30*, 4362–4366.
Cyr, R. J., & Palevitz, B. A. (1989) *Planta 177*, 245–260.
Cyr, R. J., Sotak, M., Bustos, M. M., Guiltinan, M. J., & Fosket, D. E. (1987) *Biochim. Biophys. Acta 914*, 28–34.
Dawson, P. J., & Lloyd, C. W. (1985) *EMBO J.* , 2451–2455.
de la Vina, S., Andreu, D., Medrano, F., Nieto, J. M., & Andreu, J. M. (1988) *Biochemistry 27*, 5352–5365.
Dustin, P. (1984) *Microtubules*, Springer-Verlag, Berlin.
Fosket, D. E. (1989) in *The Biochemistry of Plants* (Stumpf, P. K., & Conn, E. E., Eds.) Vol. 15, pp 393–454, Academic Press, San Diego.
Fosket, D. E., & Morejohn, L. C. (1992) *Annu. Rev. Plant Physiol. Plant Mol. Biol. 43*, 201–240.
Frigon, R. P., & Lee, J. C. (1972) *Arch. Biochem. Biophys. 153*, 587–589.
Gaskin, F., Cantor, C. R., & Shelanski, M. L. (1974) *J. Mol. Biol. 89*, 737–758.
Hamel, E., del Campo, A. A., Lowe, M. C., & Lin, C. M. (1981) *J. Biol. Chem. 256*, 11887–11894.
Hazezawa, S., Marc, J., & Palevitz, B. A. (1991) *Cell Motil. Cytoskeleton 18*, 94–106.
Johnson, K. A., & Borisy, G. G. (1975) in *Molecules and Cell Movement* (Inoue, S., & Stephens, R. E., Eds.) pp 119–141, Raven Press, New York.
Kamimura, S., & Mandelkow, E. (1992) *J. Cell Biol. 118*, 865–875.
Kim, H., Binder, L. I., & Rosenbaum, J. L. (1979) *J. Cell Biol. 80*, 266–276.
Kumar, N. (1981) *J. Biol. Chem. 256*, 10435–10441.
Laemmli, U. K. (1970) *Nature (London) 227*, 680–685.
Lataste, H., Senilh, V., Wright, M., Guenard, D., & Potier, P. (1984) *Proc. Natl. Acad. Sci. U.S.A. 81*, 4090–4094.
Lee, J. (1982) in *Methods in Cell Biology* (Wilson, L., Ed.) Vol. 24, pp 9–30, Academic Press, Inc., New York.
Levan, A. (1938) *Hereditas (Lund, Swed.) 24*, 471–486.
Manfredi, J. J., & Horwitz, S. B. (1984) *Pharmacol. Ther. 25*, 83–125.
Manfredi, J. J., Parness, J., & Horwitz, S. B. (1982) *J. Cell Biol. 94*, 688–696.
Morejohn, L. C. (1991) in *The Cytoskeletal Basis of Plant Growth and Form* (Lloyd, C. W., Ed.) pp 29–43, Academic Press Ltd., London.
Morejohn, L. C., & Fosket, D. E. (1982) *Nature (London) 297*, 426–428.
Morejohn, L. C., & Fosket, D. E. (1984a) *J. Cell Biol. 99*, 141–147.
Morejohn, L. C., & Fosket, D. E. (1984b) *Science 224*, 874–876.
Morejohn, L. C., Bureau, T. E., Tocchi, L. P., & Fosket, D. E. (1984) *Proc. Natl. Acad. Sci. U.S.A. 81*, 1440–1444.
Morejohn, L. C., Bureau, T. E., & Fosket, D. E. (1985) *Cell Biol. Int. Rep. 9*, 849–857.
Morejohn, L. C., Bureau, T. E., Mole-Bajer, J., Bajer, A. S., & Fosket, D. E. (1987a) *Planta 172*, 252–264.
Morejohn, L. C., Bureau, T. E., Tocchi, L. P., & Fosket, D. E. (1987b) *Planta 170*, 230–241.
Murashige, T., & Skoog, F. (1962) *Physiol. Plant. 15*, 473–497.
Oosawa, F., & Asakura, S. (1975) *Thermodynamics of polymerization of protein*, Academic Press Ltd., London.
Osborn, M., & Weber, K. (1982) in *Methods in Cell Biology* (Wilson, L., Ed.) Vol. 24, pp 98–129, Academic Press, Inc., New York.
Parness, J., & Horwitz, S. B. (1981) *J. Cell Biol. 91*, 479–487.
Paschal, B. M., Obar, R. A., & Vallee, R. B. (1989) *Nature (London) 342*, 569–572.
Rao, S., Horwitz, S. B., & Ringel, I. (1992) *J. Natl. Cancer Inst. 84*, 785–788.
Sackett, D. L., & Lippoldt, R. E. (1991) *Biochemistry 30*, 3511–3517.
Schiff, P. B., & Horwitz, S. B. (1981) *Biochemistry 20*, 3247–3251.
Schiff, P. B., Fant, F., & Horwitz, S. B. (1979) *Nature (London) 277*, 665–667.
Segawa, M., Kondo, K., & Ohta, S. (1981) *Phyton (Buenos Aires) 41*, 91–95.
Serrano, L., Valencia, A., Caballero, R., & Avila, J. (1986) *J. Biol. Chem. 261*, 7076–7081.
Simmonds, D. A., Seagull, R. W., & Setterfield, G. (1985) *J. Histochem. Cytochem. 33*, 345–352.
Solomon, F. (1977) *Biochemistry 16*, 358–363.
Takoudju, M., Wright, M., Chenu, J., Gueritte-Voegelein, F., & Guenard, D. (1988) *FEBS Lett. 277*, 96–98.
Thompson, W. C., Wilson, L., & Purich, D. L. (1981) *Cell Motil. Cytoskeleton 1*, 445–454.
Tiezzi, A., Moscatelli, A., Cai, G., Bartalesi, A., & Cresti, M. (1992) *Cell Motil. Cytoskeleton 21*, 132–137.
Vallee, R. B. (1982) *J. Cell Biol. 92*, 435–442.
Vallee, R. B., & Bloom, G. S. (1983) *Proc. Natl. Acad. Sci. U.S.A. 80*, 6259–6263.
Vantard, M., Schellenbaum, P., Fellous, A., & Lambert, A.-M. (1991) *Biochemistry 30*, 9334–9340.
Wang, H., Cutler, A. J., Saleem, M., & Fowke, L. C. (1989) *Eur. J. Cell Biol. 49*, 80–86.
Wani, M. C., Taylor, H. L., Wall, M. E., Coggon, P., & McPhail, A. T. (1971) *J. Am. Chem. Soc. 93*, 2325–2327.
Waxman, P. G., del Campo, A. A., Lowe, M. C., & Hamel, E. (1981) *Eur. J. Biochem. 120*, 129–136.
Wiche, G., Oberkanins, C., & Himmler, A. (1991) *Int. Rev. Cytol. 124*, 217–273.
Yadav, N. S., & Filner, P. (1983) *Planta 157*, 46–52.
Yasuhara, Y., Sonobe, S., & Shibaoka, H. (1992) *Plant Cell Physiol. 33*, 601–608.